



## Performance of CMS ECAL with first LHC data

G. Franzoni

University of Minnesota, School of Physics and Astronomy, 116 Church Street S.E. Minneapolis, MN 55455, USA

On behalf of the CMS collaboration

### ARTICLE INFO

Available online 6 July 2010

#### Keywords:

Calorimeters  
LHC  
Electromagnetic  
Lead tungstate  
Muon critical energy  
LHC beam splash  
LHC collisions

### ABSTRACT

In the Compact Muon Solenoid (CMS) experiment at the CERN Large Hadron Collider (LHC), the high resolution Electromagnetic Calorimeter (ECAL), consisting of 75 848 lead tungstate crystals and a silicon/lead preshower, will play a crucial role in the physics program. In preparation for the data taking a detailed procedure was followed to commission the ECAL readout and trigger, and to pre-calibrate, with test beam and cosmic ray data, each channel of the calorimeter to a precision of 2% or less in the central region. The first LHC collisions have been used to complete the detector commissioning and will have to provide the first *in situ* calibration. In this talk the CMS ECAL status and performance with the first collisions delivered from LHC will be reviewed.

Published by Elsevier B.V.

### 1. Introduction

The Compact Muon Solenoid (CMS) detector [1,2] is one of the two general purpose detectors installed at the CERN LHC. Its main physics goals are the observation of the Higgs boson and the search for new physics phenomena, such as particles predicted by theories beyond the Standard Model. For a mass below  $150 \text{ GeV}/c^2$ , the Higgs decay into two photons is a promising signature for the discovery. In this mass range, the Higgs width is very narrow and the signal lies above an irreducible background: this led to the choice of a high resolution electromagnetic calorimeter.

The electromagnetic calorimeter (ECAL) [1,3] of the CMS, located within a 3.8 T superconducting solenoid, is a hermetic homogeneous calorimeter comprised lead tungstate ( $\text{PbWO}_4$ ) crystals and a lead-silicon preshower. Fig. 1 shows: 61 200 crystals assembled in 36 supermodules covering the central pseudo-rapidity region  $|\eta| < 1.48$  of the barrel part (EB); two end-caps (EE) that extend the coverage up to  $|\eta| = 3$ , each comprising 7324 crystals. To gain rejection power against fake photons from neutral pion decays, a preshower detector is located in front of the crystals in the pseudo-rapidity range  $|1.65| < \eta < |2.6|$ : two lead radiators (two and one radiation length thick) initiate electromagnetic showers from the incoming photons and electrons, and silicon strip sensors placed after each radiator measure the energy deposited and the transverse shower profiles. The orientation of the strips in the two planes is orthogonal and the two planes are formed by two D-shaped structures (Dees) that join close to the vertical. Each silicon sensor measures  $63 \times 63 \text{ mm}^2$ , with an active region of  $61 \times 61 \text{ mm}^2$  and is divided into 32 strips (1.9 mm pitch).

The ECAL participates to the CMS level-one trigger decision by providing, at each LHC bunch crossing, the sum of the amplitudes recorded by a group of up to 25 crystals [4], referred to as trigger tower.

The target value for the energy resolution of the calorimeter at high energies is less than 0.5%. With these performances a Higgs boson with a mass of 120 GeV could be observed by the CMS in the gamma decay with a  $5\text{-}\sigma$  significance collecting less than  $10 \text{ fb}^{-1}$  [5].

### 2. Crystals and photodetectors

The  $\text{PbWO}_4$  allows the realisation of a compact high resolution calorimeter: its high density ( $8.3 \text{ g/cm}^3$ ) and short radiation length (8.9 mm) lead to a compact design, while its small Moliere radius (2.0 cm) permitted high granularity. The spectrum of the scintillation light peaks at 425 nm, with 80% emitted within 25 ns. The light yield, however, is low and has a temperature dependence of  $-2.2\%/^\circ\text{C}$ . The crystals have to withstand the high ionising radiation levels of the LHC environment. This causes a wavelength-dependent loss of light transmission, without changing the scintillation mechanism. The damage reaches a dose-rate dependent equilibrium resulting from the balance between damage and recovery. This effect is measured and corrected for by monitoring the optical transparency with injected light, as provided by a fibre-distributed laser system operating at two different wavelengths (440 and 796 nm). The accuracy of the correction procedure has been demonstrated in a test beam study [6] by correcting the response of the calorimeter to electrons which were recorded during an irradiation with a dose rate comparable to what is expected in the ECAL barrel at the LHC

E-mail address: [giovanni.franzoni@cern.ch](mailto:giovanni.franzoni@cern.ch)

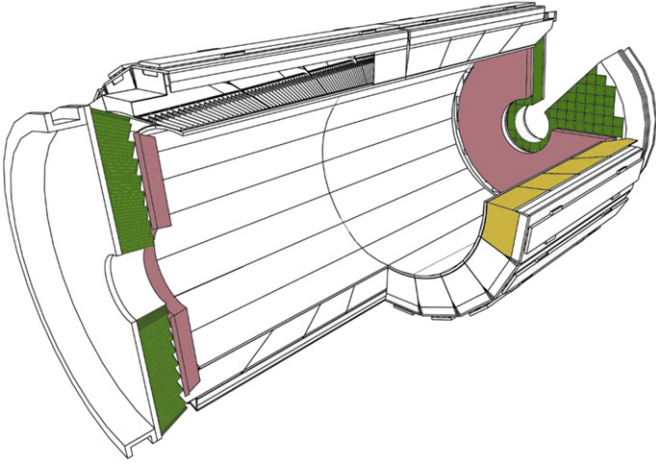


**Fig. 1.** Structure of the electromagnetic calorimeter of the Compact Muon Solenoid experiment at the CERN LHC. The supermodules composing the barrel part and the D-shaped structures composing the endcaps are visible. The preshower detector is located in front of each endcap.

luminosity of  $10^{34} \text{ cm}^2 \text{ s}^{-1}$ . Based on a few irradiated crystals, it was concluded that the ECAL response can be stabilised with an accuracy at the 0.2% level. Using data collected *in situ* during the 2008 CMS extended cosmic ray run, the stability of the correction procedure in the absence of radiation was demonstrated [7] to be better than 0.2% using the entire calorimeter.

The ECAL photo-detectors need to operate in the 3.8 T magnetic field and have a sizable gain, given the low light output of  $\text{PbWO}_4$ . In the barrel, avalanche photo-diodes (APDs) developed by Hamamatsu Photonics for the CMS, are operated at a gain of 50, exhibit a temperature coefficient of  $-2.4\%/^\circ\text{C}$  and biasing voltage coefficient of  $3\%/V$ . Radiation-resistant vacuum photo-triodes are used in the end-caps.

Because of the considerable temperature dependence both of the  $\text{PbWO}_4$  scintillation light yield and of the avalanche photo-diodes gain, the thermal stability of the CMS ECAL has to be better than  $0.1^\circ\text{C}$ . The extended 2008 run also allowed to quantify the thermal stability of the entire ECAL over a period of three weeks, resulting in a stability better than  $0.05^\circ\text{C}$  for all channels [7].

### 3. Commissioning and status

Prior to installation at the LHC, each barrel supermodule has been commissioned and pre-calibrated [8] with cosmic rays (precision of 1.5–2.5% depending on  $\eta$ ) and with test beam (0.3% for one quarter of the barrel). Laboratory measurement on the crystals and vacuum photo triodes allowed to pre-calibrate the endcaps with a precision of 7.4% [7]. The strips of the preshower have been pre-calibrated with cosmic rays to a precision of 2%.

The whole of the ECAL barrel was installed in the CMS cavern by the end of 2007, and the endcaps in the Summer of 2008. The preshower detector has been installed in the Spring 2009 and readily included in the CMS global run exercises. The whole of ECAL has been active through the 2009 LHC operations.

The health of the system is remarkable: more than 99.2% of the 76-thousand channels of the crystal ECAL are fully functional. For a large fraction (0.45%) of the channels that do not operate optimally, a coarse energy reconstruction can be performed using the trigger amplitudes generated for each tower, hence largely reducing the loss in acceptance. For the preshower, 99.7% of 137-thousand channels are perfectly operational, and no  $\eta \times \phi$  region presents problems in both planes.

The CMS data taking at the 2008 LHC operations and subsequent cosmic ray running in 2009 have allowed an extensive campaign of commissioning of the ECAL trigger. In 2009 trigger commissioning concentrated on the endcaps, remarkably more complex than the barrel due to the trigger towers approximately following an  $\eta \times \phi$  segmentation, with the mechanical and readout units segmented along  $x \times y$  instead. Ahead of the 2009 LHC beam operations the whole of the ECAL trigger was functional. Trigger amplitudes were computed correcting for channel-to-channel variations of crystal light yield and photo-multiplier gains, which is particularly important in the endcaps where there is an excursion of nearly a factor two between the intercalibrations of the innermost and outermost channels.

### 4. Calibration validation

The 2008 cosmic rays dataset has been used to measure the muon stopping power in  $\text{PbWO}_4$  over the momentum range from 5 to 1000 GeV/c [9], yielding the first measurement of the muon critical energy:  $160_{-6}^{+5} (\text{stat.}) \pm 8 (\text{syst.}) \text{ GeV}$ .

The stopping power measurement was also used to validate *in situ* the ECAL pre-calibration constants of 14 of the 36 barrel supermodules as a function of  $\eta$ , by comparing the stopping power ( $dE/dx$ ) distributions across different  $\eta$  regions [7]. This is important because procedures for *in situ* calibration at LHC will provide inter-calibration of crystals within rings at constant  $-\eta$ , and at startup the pre-calibration will provide the relative scale for crystals located in different rings. Muons were selected to have momentum between 5 and 10 GeV/c (where energy loss is dominated by ionisation), to pass through the CMS tracker volume, and to form an angle of less than  $30^\circ$  with the traversed crystal axis. Energy deposits in the bottom hemisphere of ECAL were corrected for the momentum variation due to the energy released in the top part. Fig. 2 shows the truncated mean  $dE/dx$  as a function of the crystal index in the  $\eta$  coordinate, normalised to the average  $dE/dx$ . The distribution is shown over the range  $-0.7 < \eta < 0.7$ , where most of the muons passing the selections are located. The RMS spread of the measurements, indicating the precision to which the  $\eta$ -dependent pre-calibration scale is verified, is 0.8%. The statistical precision of each measurement (error bars on the points) is typically 0.4%. The total systematic uncertainty represented by the shaded region is 0.5%. The main contribution to the systematic

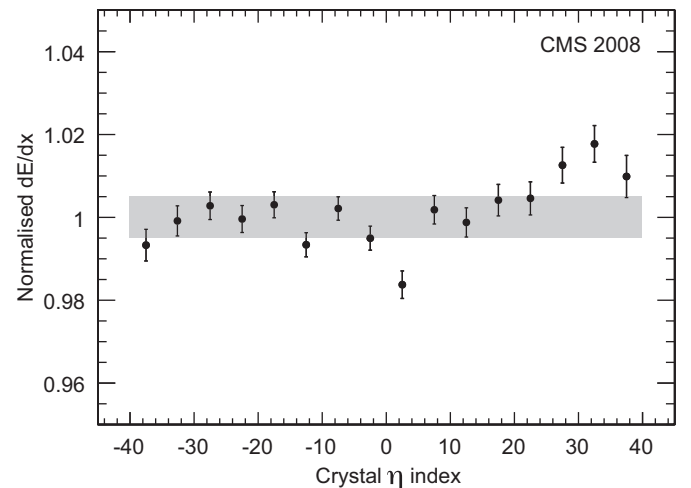


**Fig. 2.** Mean stopping power,  $dE/dx$ , versus the crystal index along the pseudorapidity ( $\eta$ ). Data points are the averages over five crystals rings in  $\eta$  at all values of  $\phi$ . The shaded region represents the systematic uncertainty on the measurement of  $dE/dx$ .

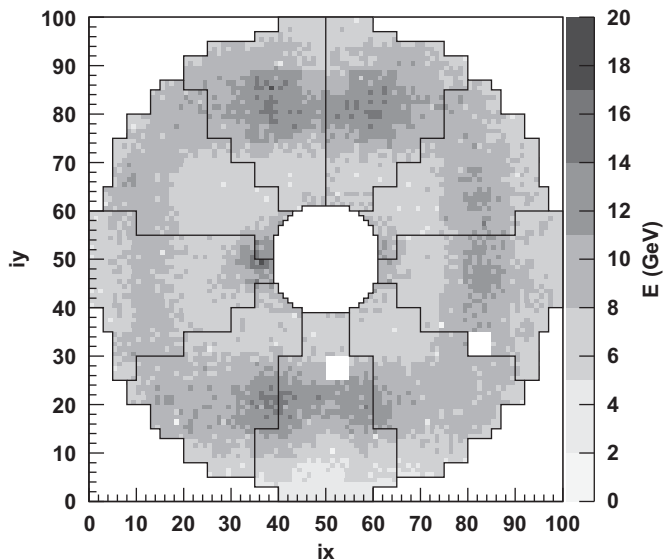


**Fig. 3.** Average recorded signal in GeV per crystal deposited in the negative side of the ECAL endcap over 800 splashes. Each bin represents one crystal. The white regions were excluded from the readout.

error is the energy scale dependence on the angle between the muon trajectory and the crystal axis (0.5%).

## 5. Beam splashes

While preparing colliding beams in the Autumn 2009, the LHC delivered to the CMS over nine-hundred beam “splash” events, when one of the beams was deliberately addressed onto collimators located 150 m away from the CMS interaction point resulting in muons which reached the cavern and traversed horizontally the CMS detector. Splashes allowed to consolidate the CMS readout and trigger latencies, to validate the ECAL single-channel time alignment (derived in 2008 with a precision of 500 ps [10]) and to deploy new time alignments (to be published in the near future). The CMS relied on the trigger information generated by the central region of the ECAL barrel ( $|\eta| < 0.44$ ) to trigger the readout of the splash events, confident of its functionality and of the accuracy of its internal synchronisation. The average calibrated energy recorded over about eight-hundred events by the upstream ECAL endcap crystals is shown in Fig. 3, ranging between 6 and 12 GeV. The modulation results from a combination of splash energy flow and CMS geometrical effects: the central square structure and the deficit at the bottom are interpreted as due, respectively, to the presence of shielding material and the floor of the LHC tunnel. The map of the amplitudes recorded in one event by the inner plane of the upstream preshower is shown in Fig. 4. The fluence modulations are consistent with the energy maps seen in the ECAL crystals, and isolated hot spots, observed consistently across two preshower planes, are attributed to muon bremsstrahlung. The crystals and the preshower consistently yield an estimated fluence of muons of  $5 \text{ cm}^{-2}$ .

The 2008 splash events have been used to validate and improve the ECAL endcap intercalibrations [7]. The procedure consists of three steps: firstly  $5 \times 5$  arrays of crystals are cross-calibrated by averaging 25 laboratory pre-calibrations, thus accounting for the radial inter-calibration dependence and the modulations of the splash fluence. Then the assumption is made that the fluence of splash charged particles is uniform within the  $5 \times 5$  array. Intercalibrations can finally be derived by equalising the response over an entire endcap. The precision of these intercalibrations is measured to be 10.4% by comparison to an independent set in the

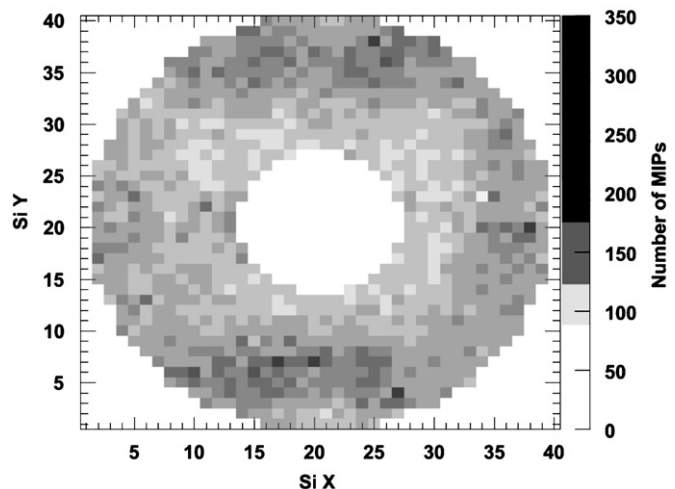


**Fig. 4.** Recorded signal (m.i.p. equivalent) in the negative inner plane of the ECAL preshower in one splash event. Each bin represents one sensor (32 strips).

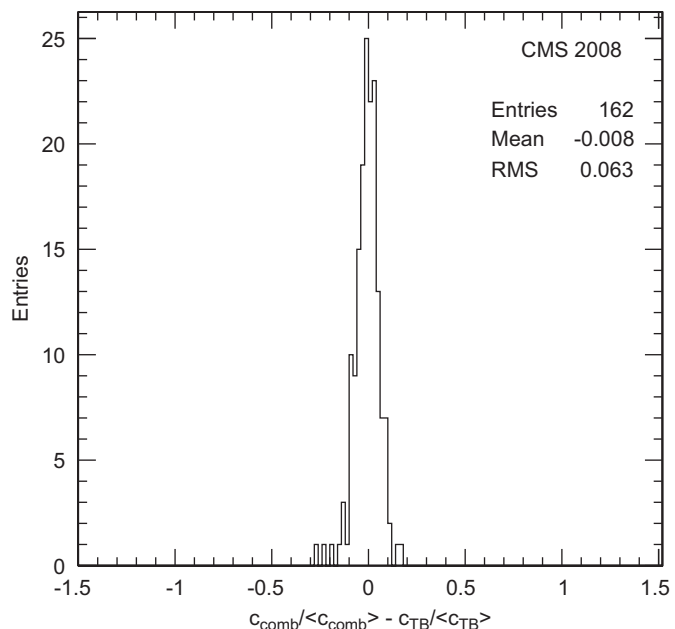


**Fig. 5.** For the ECAL endcap, comparison between the combination of splash-derived intercalibrations and laboratory pre-calibrations to precalibration obtained at test beam with electrons.

region which was calibrated also with an electron beam. An error-weighted combination of laboratory pre-calibration and splash calibration has been provided and compared to the test beam set for a reference sample of 162 crystals. Fig. 5 shows an improvement in the RMS from 7.4% to 6.3% after the combination, indicating that the coefficients from the laboratory and the splashes are to a good extent independent. An inter-calibration analysis with the 2009 splashes, taking advantage also of the preshower to measure the muon fluence leads to a further improvement in the combination (and will be published in the near future).

## 6. LHC collisions

Starting on November 23rd 2009, LHC delivered proton–proton collisions to the experiments at the SPS injection energy of 900 GeV

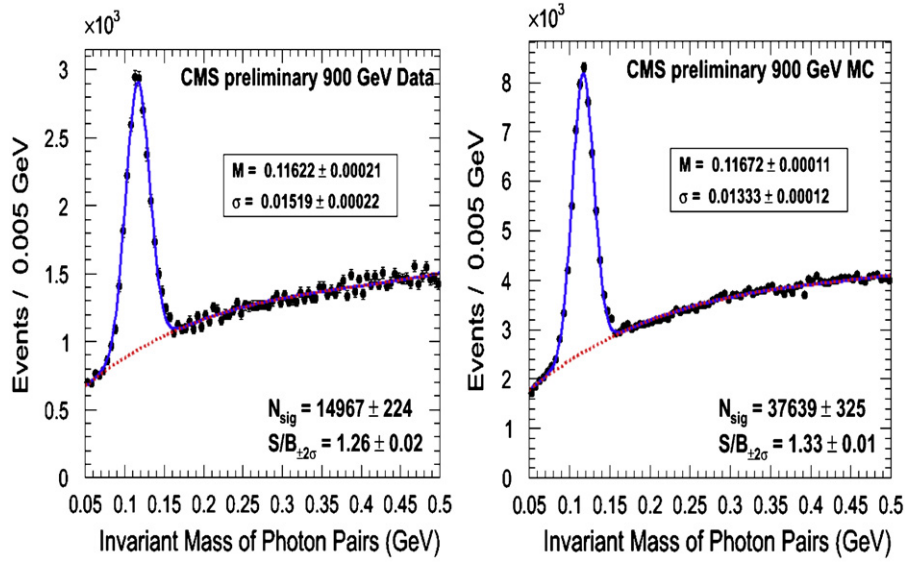


Fig. 6. Uncorrected invariant mass distributions of ECAL cluster pairs selected as described in the text. Left: proton–proton collision data. Right: Monte Carlo simulation.

in the centre of mass. Hits reconstructed in the ECAL endcaps with energy deposits matching across the two preshower planes and crystals were among the very first evidences that collisions were actually occurring at the CMS. After the first three days of collisions, the observation of the  $\pi^0$  peak was established in the di-cluster invariant mass distribution. Three simple selections were applied to pairs of  $3 \times 3$  crystals clusters in the ECAL barrel: a minimum transverse energy for either photon candidate  $E_T(\gamma_{1,2}) > 0.3$  GeV, a minimum transverse energy for the di-photon system  $E_T(\pi^0) > 0.9$  GeV and a shower shape cut  $E_4/E_9 > 0.85$ , enhancing electromagnetic showers ( $E_9$  being the  $3 \times 3$  cluster energy and  $E_4$  the largest of the four  $2 \times 2$  sub-cluster energies). Fig. 6 shows the invariant mass distributions as obtained from collision data and Monte Carlo simulation of minimum bias events. A fair agreement is found between the two in the peak position and width, signal to background ratio and background shape. The cluster energies used to compute the invariant mass are corrected neither for the incomplete shower containment of  $3 \times 3$  crystals matrices nor for the effect of online zero suppression, which removes from the data crystals with energy deposits less than 100 MeV. Both these effects conspire to a peak position lower than the nominal  $\pi^0$  mass (0.135 GeV [11]). By applying Monte Carlo-derived corrections, the mass peak moves to within 2% of the nominal  $\pi^0$  mass. Tighter selections on the same variables have allowed the  $\pi^0$  observation also on the ECAL endcaps, as well as the observation of the  $\eta$  meson. The collection of the  $\pi^0$  candidates has been particularly useful to start the commissioning the inter-calibration technique which relies on the  $\pi^0$  mass constraint to align the response of the ECAL channels [8].

For the first days of collision data taking the CMS relied on beam scintillator counters and beam pick-up devices for minimum bias trigger. The first level-one trigger algorithms relying on sub-detectors of the CMS to be activated were the ECAL-based electron-gamma paths, after having assessed the correctness of the latency and internal alignment of the ECAL trigger towers.

## 7. Conclusions

In 2008 and 2009 the CMS electromagnetic calorimeter has gone through the completion of the installation, commissioning and pre-calibration. The health of the system is remarkable and precision of inter-calibration (1.5–2.5% for EB, 6.3% for EE and 2% for ES) already acceptable for the majority of the early physics

analyses. The ECAL has successfully recorded proton-proton collision events delivered by the LHC, observed the  $\pi^0$  meson and is ready to further improve its *in situ* performances to participate at best in the CMS physics program.

## Acknowledgements

We wish to congratulate our colleagues in the CERN accelerator departments for the excellent performance of the LHC machine. We thank the technical and administrative staff at CERN and other CMS Institutes, and acknowledge support from: FMSR (Austria); FNRS and FWO (Belgium); CNPq, CAPES, FAPERJ, and FAPESP (Brazil); MES (Bulgaria); CERN; CAS, MoST, and NSFC (China); COLCIENCIAS (Colombia); MSES (Croatia); RPF (Cyprus); Academy of Sciences and NICPB (Estonia); Academy of Finland, ME, and HIP (Finland); CEA and CNRS/IN2P3 (France); BMBF, DFG, and HGF (Germany); GSRT (Greece); OTKA and NKTH (Hungary); DAE and DST (India); IPM (Iran); SFI (Ireland); INFN (Italy); NRF (Korea); LAS (Lithuania); CINVESTAV, CONACYT, SEP, and UASLP-FAI (Mexico); PAEC (Pakistan); SCSR (Poland); FCT (Portugal); JINR (Armenia, Belarus, Georgia, Ukraine, Uzbekistan); MST and MAE (Russia); MSTDS (Serbia); MICINN and CPAN (Spain); Swiss Funding Agencies (Switzerland); NSC (Taipei); TUBITAK and TAEK (Turkey); STFC (United Kingdom); DOE and NSF (USA). Individuals have received support from the Marie-Curie IEF program (European Union); the Leventis Foundation; the A. P. Sloan Foundation; and the Alexander von Humboldt Foundation. The author is grateful all the collaborators of the CMS experiment, and in particular the ECAL group, for having designed, built and operated the detector making these results possible. A special acknowledgement to Dr. P. Meridiani and Prof. T. Tabarelli de Fatis: the author learnt immensely from them both during the last two years as CMS ECAL performance co-conveners.

## References

- [1] The CMS Collaboration, J. Instr. 3 (2008) S08004.
- [2] The CMS Collaboration, CMS Physics Technical Design Report, Volume 1: Detector Performance and Software, CERN-LHCC-2006-001, 2006.
- [3] The CMS Collaboration, The Electromagnetic Calorimeter Technical Design Report, CERN/LHCC 97-033, 1997.
- [4] P. Paganini, J. Phys. Conf. Ser. 160 (2009) 012062.
- [5] The CMS Collaboration, J. Phys. G Nucl. Part. Phys. 34 (2007) 995.

- [6] A. Ghezzi, et al., Analysis of the response evolution of the CMS electromagnetic calorimeter under electron and pion irradiation, CMS NOTE 2006/038, 2006.
- [7] The CMS Collaboration, Performance and operation of the CMS electromagnetic calorimeter, J. Instr. 5 T03010, 2010, doi:10.1088/1748-0221/5/03/T03010.
- [8] The CMS ECAL Group, J. Instr. 3 (2008) P10007.
- [9] The CMS Collaboration, Measurement of the muon stopping power in lead tungstate, J. Instr. 5 P03007, 2010, doi:10.1088/1748-0221/5/03/P03007.
- [10] The CMS Collaboration, Time reconstruction and performance of the CMS electromagnetic calorimeter, arXiv:0911.4044, J. Instr., accepted for publication.
- [11] C. AMSLER, et al., Particle Data Group, Phys. Lett. B 667 (2008) 1.